

# Extremely high electron mobility in isotopically-enriched $^{28}\text{Si}$ two-dimensional electron gases grown by chemical vapor deposition

Jiun-Yun Li,<sup>1,(a)</sup> Chiao-Ti Huang,<sup>1</sup> Leonid P. Rokhinson,<sup>2</sup> and James C. Sturm<sup>1</sup>

<sup>1</sup>Department of Electrical Engineering and Princeton Institute for the Science and Technology of Materials, Princeton University, Princeton, New Jersey 08544, USA

<sup>2</sup>Department of Physics, Purdue University, West Lafayette, Indiana 47907, USA

(Received 26 July 2013; accepted 25 September 2013; published online 16 October 2013)

Both depletion-mode and enhancement-mode two-dimensional electron gases (2DEGs) in isotopically enriched  $^{28}\text{Si}$  with extremely high mobility ( $522\,000\text{ cm}^2/\text{Vs}$ ) are presented. The samples were grown by chemical vapor deposition using enriched silane. The fraction of the spin-carrying isotope  $^{29}\text{Si}$  was reduced to the level of 800 ppm by  $^{28}\text{Si}$  enrichment, with the electron spin dephasing time expected to be as long as  $2\,\mu\text{s}$ . Remote impurity charges from ionized dopants and the  $\text{Si}/\text{Al}_2\text{O}_3$  interface were suggested to be the dominant source for electron scattering in the enriched  $^{28}\text{Si}$  2DEGs. © 2013 AIP Publishing LLC. [<http://dx.doi.org/10.1063/1.4824729>]

Quantum dots (QDs) containing single electrons are very promising for the realization of spin-based quantum computing in solid-state systems due to the maturity of semiconductor technology.<sup>1</sup> The short dephasing time  $T_2^* \sim 7\text{ ns}$  of electron spins<sup>2</sup> in GaAs QDs due to the strong hyperfine interactions with the host nuclei<sup>3</sup> imposes an upper limit on the duration of a gate switching event, in order to preserve the quantum phase information before a gate switching operation is completed. A longer dephasing time ( $\sim 360\text{ ns}$ ) of electron spins was demonstrated<sup>4</sup> in silicon with a natural abundance of the  $^{29}\text{Si}$  isotope (4.7%), which carries nuclear spins.<sup>5</sup>

To go beyond the limit of natural Si, in this Letter, we report depletion- and enhancement-mode Si two-dimensional electron gases (2DEG) with the  $^{29}\text{Si}$  depleted to only 1.7% of its natural abundance, for an absolute level of 0.08%. The transport properties were measured at cryogenic temperatures, with a high mobility of  $522\,000\text{ cm}^2/\text{Vs}$ , among the best reported of any type of modulation-doped Si 2DEGs grown by chemical vapor deposition (CVD). Based on a model of spin decoherence in Si,<sup>6</sup> we estimated the upper limit of spin dephasing time to be  $2\,\mu\text{s}$  in such structures.

In this work, polished relaxed  $\text{Si}_{0.73}\text{Ge}_{0.27}$  buffers with a graded  $\text{Si}_{1-x}\text{Ge}_x$  layer ( $0 < x < 0.27$ ) and a  $\text{Si}_{0.73}\text{Ge}_{0.27}$  layer grown on Si (100) substrates were used for the epitaxial growth of silicon 2DEGs. The preparation steps of wafers and the precursors for epitaxial growth were described elsewhere.<sup>7</sup> After cleaning steps, a SiGe relaxed buffer layer of 100–150 nm was grown at  $575^\circ\text{C}$ , followed by a strained-Si layer (2DEG layer) at  $625^\circ\text{C}$ , a SiGe setback layer at  $575^\circ\text{C}$ , a n-type SiGe supply layer at  $575^\circ\text{C}$ , and a SiGe cap layer at  $575^\circ\text{C}$ , followed by a strained Si cap layer at  $625^\circ\text{C}$  (Table I) for depletion-mode 2DEGs. All layers above the polished relaxed buffers were grown using diluted silane of enriched  $^{28}\text{Si}$  with respect to other isotopes. For enhancement-mode 2DEGs, the structure was the same, except that there was no setback or doped layer, the SiGe cap was either 60 or 150 nm,

and the enriched silane was used only for the growth of Si quantum well.

The concentrations of three isotopes,  $^{28}\text{Si}$ ,  $^{29}\text{Si}$ , and  $^{30}\text{Si}$ , and Ge, vs. depth in a depletion mode sample are shown in Fig. 1. Below the growth interface at a depth of 185 nm, the fractions of  $^{28}\text{Si}$ ,  $^{29}\text{Si}$ , and  $^{30}\text{Si}$  are 92, 4.7, and 3.3%, respectively, which are the natural isotopic abundances of silicon.<sup>5</sup> For Si and SiGe epitaxial layers grown with silane of enriched  $^{28}\text{Si}$ , the fractions for those three isotopes become 99.72, 0.08, and 0.002%, respectively. The ratios of  $^{28}\text{Si}$  to  $^{29}\text{Si}$ , are 20 and 1250 in the natural and enriched silicon, respectively (a  $60\times$  increase). The  $^{28}\text{Si}$  to  $^{30}\text{Si}$  ratio increases from 27 to 50 000 ( $2000\times$  increase). The electron transport properties of Si 2DEG samples were characterized by low-temperature Hall measurement (at 4 K and 0.3 K). For the depletion-mode device, the sample was first mesa-etched to define a Hall bar geometry, and then Ohmic contacts were made by AuSb (1% Sb) deposition followed by rapid thermal annealing at  $450^\circ\text{C}$  for 10 min. For enhancement-mode devices, Ohmic contacts were first made by ion implantation of phosphorus followed by furnace annealing at  $600^\circ\text{C}$  for 1 h.<sup>8</sup> Then, an  $\text{Al}_2\text{O}_3$  gate insulator of 90 nm was deposited at  $300^\circ\text{C}$  by atomic layer deposition (ALD) with a metal gate of Cr/Au on top. Longitudinal resistance ( $R_{xx}$ ) and Hall resistance ( $R_{xy}$ ) were measured at 4 K for all samples and at 0.3 K for the depletion-mode device using the low-frequency ac lock-in technique.

Before growing device structures with the isotopically-enriched silane, we grew depletion-mode structures with normal silane to find densities and structures with high mobility. The sample structure and growth conditions were similar to those in Table I, although the SiGe setback thickness and other layers were varied slightly. A summary plot of Hall mobility vs. density at 4 K from ungated Hall bars is shown in Fig. 2, with squares representing the data from unenriched silane. Highest mobilities were observed in the density range of  $4\text{--}6 \times 10^{11}\text{ cm}^{-2}$ . Below this density (achieved with a thicker SiGe setback layer), the decreasing electron mobility results from less electron screening, which is a stronger (negative) effect than the positive effect of moving the ionized dopants farther from the 2DEG. A dotted line fit to the data

<sup>a)</sup>Present address: Department of Electrical Engineering and Graduate Institute of Electronics Engineering, National Taiwan University, Taipei 10617, Taiwan. Electronic mail: [jiunyun@ntu.edu.tw](mailto:jiunyun@ntu.edu.tw)

TABLE I. Epitaxial layer structures and growth temperatures of depletion-mode and enhancement-mode enriched  $^{28}\text{Si}$  2DEG samples.

Layer (nm)	Growth temperature ( $^{\circ}\text{C}$ )	Depletion-mode (modulation-doped)	Enhancement-mode (undoped)
Si cap	625	7	3
SiGe cap	575	25	60 or 150
SiGe supply	575	10	0
(P doping level)		$(4 \times 10^{18} \text{ cm}^{-3})$	(no doping)
SiGe setback	575	25	0
Si quantum well	625	16	9 <sup>a</sup>
SiGe re-growth	575	110	150

<sup>a</sup>For enhancement-mode devices,  $^{28}\text{Si}$  was enriched only in the Si quantum well layer.

shows a relationship of  $\mu \propto n^{1.5}$ . This is consistent with prior work<sup>9,10</sup> which suggested that with an exponent of 1.5, remote impurity scattering from the modulation-doped supply layer is the dominant scattering mechanism at low densities. On the other hand, as the electron density increases above  $6 \times 10^{11} \text{ cm}^{-2}$  (by reducing the setback distance), the mobility drops. This has been attributed to the stronger scattering induced by a shorter setback distance, which compromises the effects of electron screening.<sup>11</sup>

The depletion-mode samples with enriched  $^{28}\text{Si}$  were designed to have a density in the range of maximum mobility as shown in Fig. 2 ( $4\text{--}6 \times 10^{11} \text{ cm}^{-2}$ ). The data points of these samples are plotted as stars in Fig. 2, along with the data for the natural Si 2DEGs. The trends of mobility vs. density are remarkably consistent, with the exception of one sample for unknown reasons. The highest Hall mobility observed among enriched- $^{28}\text{Si}$  samples at 4 K was  $399\,000 \text{ cm}^2/\text{V s}$  with a density of  $4 \times 10^{11} \text{ cm}^{-2}$ .

One sample (that of Table I) was chosen for measurements at 0.3 K. At 4 K, its Hall electron density is  $4 \times 10^{11} \text{ cm}^{-2}$  and the Hall mobility is  $399\,000 \text{ cm}^2/\text{V s}$ . At 0.3 K, the longitudinal ( $R_{xx}$ ) and transverse (Hall) resistances ( $R_{xy}$ ) were also measured with the magnetic field up to 8 T (Fig. 3). The onset of Shubnikov-de Haas (SdH) oscillations in  $R_{xx}$  occurs at 0.4 T. The spin splitting due to the associated Zeeman energy difference exceeding the Landau level broadening occurs at 0.75 T with a filling factor of  $\nu = 24$ .

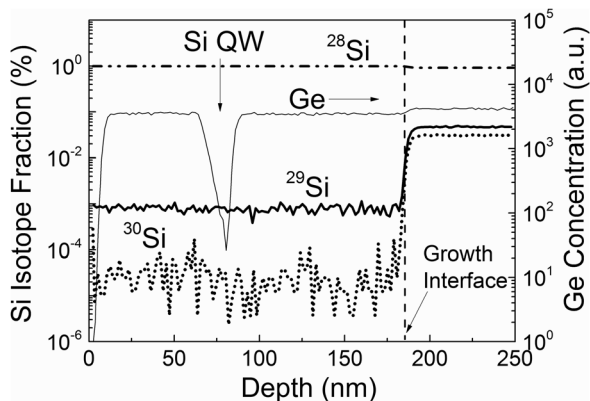


FIG. 1. Concentrations of silicon isotopes  $^{28}\text{Si}$ ,  $^{29}\text{Si}$ , and  $^{30}\text{Si}$ , and Ge vs. depth in a 2DEG structure by SIMS measurements. The growth was started at a depth of 185 nm, and the Si QW is at a depth of 75 nm.

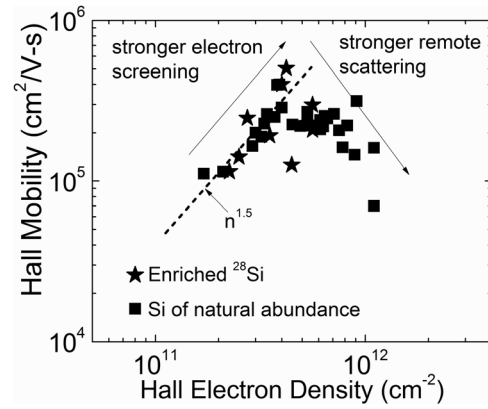


FIG. 2. Hall electron mobility vs. density for various ungated depletion-mode (modulation-doped) Si 2DEGs grown in our lab. Stars represent the data of isotopically-enriched  $^{28}\text{Si}$  2DEGs and squares are the data from Si 2DEGs of natural isotopic abundance.

The revelation of two-fold degeneracy from two valleys of density of states was observed at 1.9 T with  $\nu = 9$ . For Hall resistance ( $R_{xy}$ ), the quantum Hall structures can be resolved at  $B = 0.7 \text{ T}$  at  $\nu = 24$  and clear plateaus were observed at  $\nu = 2, 4, 8$ , etc. The two-dimensional electron densities extracted from SdH oscillations and low-field Hall resistance were  $4.02$  and  $4.18 \times 10^{11} \text{ cm}^{-2}$ , respectively showing that parallel conduction is insignificant. The electron mobility of this device at 0.3 K is  $522\,000 \text{ cm}^2/\text{V s}$ , corresponding to an associated mean free path of  $6 \mu\text{m}$ . This mobility may be the highest reported for modulation-doped Si 2DEGs grown by CVD regardless of  $^{28}\text{Si}$  enrichment. In previous work of isotopically-enriched  $^{28}\text{Si}$  2DEGs grown by molecular beam epitaxy, the highest reported mobility was  $55\,000 \text{ cm}^2/\text{V s}$ .<sup>12</sup>

Enhancement-mode samples with enriched  $^{28}\text{Si}$  only in the Si QW layer were made without n-type dopants with a SiGe setback layer of 60 or 150 nm on top of the 2DEG layer (Table I). With a metal gate of Cr/Au on top of 90-nm  $\text{Al}_2\text{O}_3$ , the Hall electron density increased with gate voltage and mobility increased rapidly with electron density (Fig. 4). The effective gate capacitance extracted from the slopes of  $n_{2D}$  vs.  $V_g$  are  $5.8 \times 10^{-8} \text{ F/cm}^2$  and  $4.1 \times 10^{-8} \text{ F/cm}^2$  for the setback layers of 60 and 150 nm (Fig. 4(a)), respectively, within 5% of the calculated values based on a parallel-plate capacitor model. The lowest densities are 1.1 and

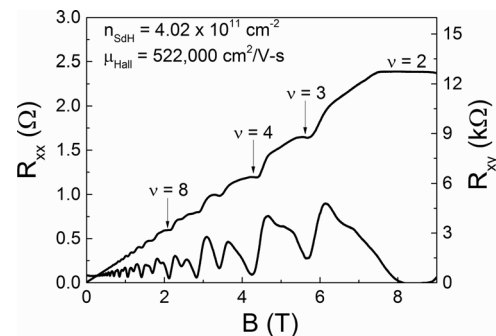


FIG. 3. Magneto-resistances of a depletion-mode enriched  $^{28}\text{Si}$  2DEG device measured at 0.3 K. Electron density ( $4 \times 10^{11} \text{ cm}^{-2}$ ) and mobility ( $522\,000 \text{ cm}^2/\text{V s}$ ) were extracted from the periods of Shubnikov-de Haas oscillations in longitudinal resistance ( $R_{xx}$ ) vs.  $(1/B)$  and its value at zero field.

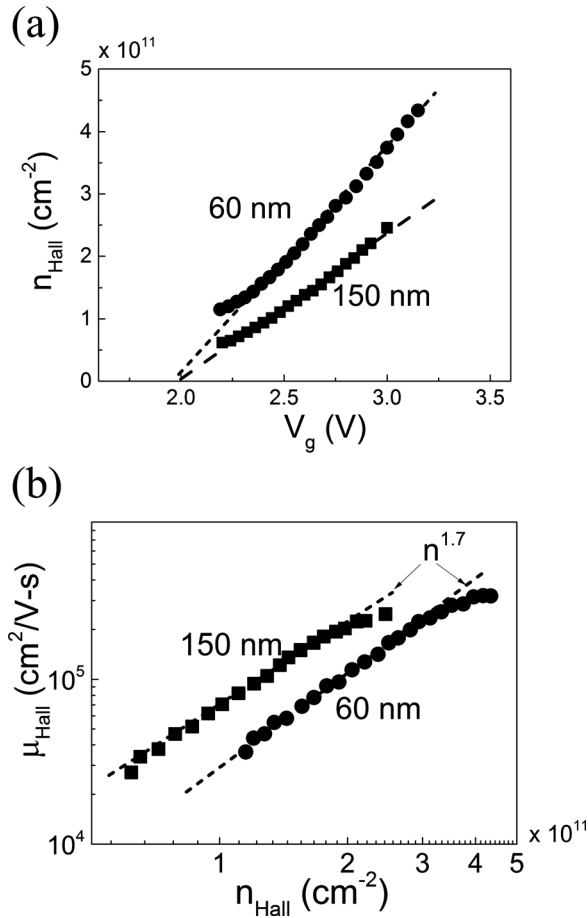


FIG. 4. (a) Electron density vs. gate voltage by Hall measurement at 4 K for enhancement-mode enriched  $^{28}\text{Si}$  2DEGs with a SiGe cap layer of 60 or 150 nm, and (b) mobility vs. density for these two devices at 4 K, along with dotted lines representing a power law relation between mobility and density. The lowest observed density was  $6 \times 10^{10} \text{ cm}^{-2}$  for a 150 nm SiGe cap layer.

$0.6 \times 10^{11} \text{ cm}^{-2}$  at  $V_g = 2.2 \text{ V}$ , which we believe is the lowest density among all reported enriched  $^{28}\text{Si}$  2DEGs. At lower gate voltages, there was no conduction in the 2DEG channel because of the metal-insulator transition (MIT).<sup>13</sup>

In the enhancement-mode devices without  $^{28}\text{Si}$  enrichment, a higher mobility is possible by increasing the SiGe setback layer between Si surface and the 2DEG layer.<sup>14</sup> However, we chose our structures of 60 to 150 nm because a thickness of  $\sim 100 \text{ nm}$  is preferred for the precise lateral gate control over the underlying 2DEG for quantum dot applications. In both samples, the mobility scales with the density as  $\mu \propto n^{1.7}$ . This is close to the exponent of 1.5 in a theoretical model<sup>8</sup> when the 2DEG mobility is limited by the remote impurity scattering. In contrast, when the background impurity scattering dominates, the exponent is expected to be unity.<sup>8</sup> Thus, the mobility in the enhancement mode devices appears to be limited by remote impurity scattering, presumably impurity charges at the Si/ $\text{Al}_2\text{O}_3$  interface.

We now estimate the potential impact of a  $^{29}\text{Si}$  level of 0.08% on electron decoherence in Si QDs. By reducing the  $^{29}\text{Si}$  level to  $< 50 \text{ ppm}$ , a lower spin decoherence rate of electrons bound to phosphorus donors in isotopically enriched  $^{28}\text{Si}$  has been demonstrated experimentally.<sup>15</sup> In QDs, a similar effect is expected. Assuming a Si QD of  $10^5$  nuclei Assali *et al.*<sup>6</sup> have predicted a dephasing time  $T_2^*$  given by

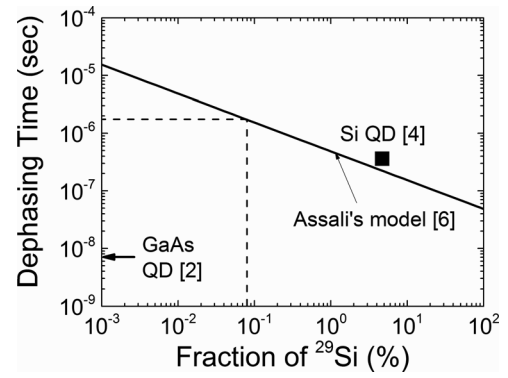


FIG. 5. Dephasing time of electron spins in silicon quantum dots vs.  $^{29}\text{Si}$  fraction. The solid line is the model prediction by Assali,<sup>6</sup> and the solid square represents data in QDs made in naturally occurring-Si.<sup>4</sup> If the spin decoherence was due solely to nuclear hyperfine interactions, the expected dephasing time for a  $^{29}\text{Si}$  fraction of 0.08% (dotted lines,  $^{29}\text{Si}$  level of this work) would be  $2 \mu\text{s}$ . The dephasing time ( $\sim 7 \text{ ns}$ ) of GaAs QDs<sup>2</sup> is also shown for comparison.

$$T_2^* = \frac{10^{11} \hbar}{4.3 eV \cdot \sqrt{10^5 r}}, \quad (1)$$

where  $r$  is the atomic fraction of  $^{29}\text{Si}$ . The predicted dephasing time versus  $r$  is shown in Fig. 5 and compared with experimental results. Maune *et al.* reported a dephasing time of 360 ns in double QDs in Si of natural abundance,<sup>4</sup> which is very close to Assali's model prediction. In our samples, the fraction of  $^{29}\text{Si}$  is  $\sim 0.08\%$  (vertical line in Fig. 5) and the dephasing time is expected to be  $2 \mu\text{s}$ . For comparison, a much shorter dephasing time of 7 ns in GaAs QDs<sup>2</sup> was also labeled, showing a great promise of isotopically-enriched  $^{28}\text{Si}$  2DEGs for achieving low electron spin decoherence rates in Si QDs.

In summary, we report high quality depletion-mode and enhancement-mode 2DEGs in silicon grown by CVD from silane in which the  $^{29}\text{Si}$  level was reduced to 0.08%. Such a level may lead to an electron dephasing time in silicon quantum dots as long as  $2 \mu\text{s}$ . A mobility of  $522\,000 \text{ cm}^2/\text{V}\cdot\text{s}$  was observed in a depletion-mode device. In enhancement-mode devices, a low electron density of  $6 \times 10^{10} \text{ cm}^{-2}$  before the metal-insulator transition was demonstrated by gating. In both depletion- and enhancement-mode devices, a strikingly similar dependence of mobility on density was seen, suggesting remote impurities limit the mobility in both cases.

This work at Princeton University was sponsored by United States Department of Defense through DARPA) and through ARO (project W911NF-09-1-0498), and by the NSF MRSEC program (DMR-0819860). The views and conclusions contained in this document are those of the authors and should not be interpreted as representing the official policies, either expressly or implied, of the U.S. Government. We also thank Amberwave Semiconductor for supplying the relaxed  $\text{Si}_{0.7}\text{Ge}_{0.3}$  buffers.

<sup>1</sup>M. A. Eriksson, M. Friesen, S. N. Coppersmith, R. Joynt, L. J. Klein, K. Slinker, C. Tahan, P. M. Mooney, J. O. Chu, and S. J. Koester, *Quantum Inf. Process.* **3**, 133 (2004).

<sup>2</sup>J. R. Petta, A. C. Johnson, J. M. Taylor, E. A. Laird, A. Yacoby, M. D. Lukin, C. M. Marcus, M. P. Hanson, and A. C. Gossard, *Science* **309**, 2180 (2005).

- <sup>3</sup>T. D. Ladd, F. Jelezko, R. Laflamme, Y. Nakamura, C. Monroe, and J. L. O'Brien, *Nature* **464**, 45 (2010).
- <sup>4</sup>B. M. Maune, M. G. Borselli, B. Huang, T. D. Ladd, P. W. Deelman, K. S. Holabird, A. A. Kiselev, I. Alvarado-Rodriguez, R. S. Ross, A. E. Schmitz, M. Sokolich, C. A. Watson, M. F. Gyure, and A. T. Hunter, *Nature* **481**, 344 (2012).
- <sup>5</sup>D. R. Lide, *CRC Handbook of Chemistry and Physics* (CRC, 2006).
- <sup>6</sup>L. V. C. Assali, H. M. Petrilli, R. B. Capaz, B. Koiller, X. Hu, and S. Das Sarma, *Phys. Rev. B* **83**, 165301 (2011).
- <sup>7</sup>J. Y. Li, C. T. Huang, L. P. Rokhinson, and J. C. Sturm, *ECS Trans.* **50**, 145 (2013).
- <sup>8</sup>C. T. Huang, J. Y. Li, and J. C. Sturm, *IEEE Elec. Dev. Lett.* **34**, 21 (2013).
- <sup>9</sup>D. Monroe, Y. H. Xie, E. A. Fitzgerald, P. J. Silverman, and G. P. Watson, *J. Vac. Sci. Technol. B* **11**, 1731 (1993).
- <sup>10</sup>D. Larocche, D. Das Sarma, G. Gervais, M. P. Lilly, and J. L. Reno, *Appl. Phys. Lett.* **96**, 162112 (2010).
- <sup>11</sup>J. J. Heremans, M. B. Santos, K. Hirakawa, and M. Shayegan, *J. Appl. Phys.* **76**, 1980 (1994).
- <sup>12</sup>A. Wild, J. Kierig, J. Sailer, J. W. Ager III, E. E. Haller, G. Abstreiter, S. Ludwig, and D. Bougeard, *Appl. Phys. Lett.* **100**, 143110 (2012).
- <sup>13</sup>S. V. Kravchenko and M. P. Sarachik, *Rep. Prog. Phys.* **67**, 1 (2004).
- <sup>14</sup>S.-H. Huang, T. M. Lu, S.-C. Lu, C.-H. Lee, C. W. Liu, and D. C. Tsui, *Appl. Phys. Lett.* **101**, 042111 (2012).
- <sup>15</sup>A. M. Tyryshkin, S. Tojo, J. J. L. Morton, H. Riemann, N. V. Abrosimov, P. Becker, H.-J. Pohl, T. Schenkel, M. L. W. Thewalt, K. M. Itoh, and S. A. Lyon, *Nature Mater.* **11**, 143 (2012).